Effect of modulated antiparallel domain patterns on the dielectric permittivity in epitaxial $Bi_2Ti_4O_{11}$-$Bi_4Ti_3O_{12}$ films

A. Q. Jiang, Z. H. Chen, F. Chen, Y. L. Zhou, M. He, and G. Z. Yang
Laboratory of Optical Physics, Institute of Physics, Chinese Academy of Sciences, Beijing 100080, People's Republic of China
(Received 6 June 2000; revised manuscript received 5 September 2000; published 14 February 2001)

We have used the pulsed laser deposition technique to grow a series of *c*-axis oriented $x\,Bi_2Ti_4O_{11}$-$(1-x)Bi_4Ti_3O_{12}$ films at the morphotropic phase boundary on $LaNiO_3$ electroded $SrTiO_3$ (100) substrates. The films are alternative stacking of ferroelectric $Bi_4Ti_3O_{12}$ and $Bi_2Ti_4O_{11}$ layers. *P-E* hysteresis loop and capacitance versus voltage measurements show antiparallel domain orientations with adjacent $Bi_4Ti_3O_{12}$ and $Bi_2Ti_4O_{12}$ layers, which enhances the dielectric permittivity of ferroelectric capacitors considerably. Raman studies indicate different symmetry phases of constituent $Bi_4Ti_3O_{12}$ in $Bi_2Ti_4O_{11}$ and $Bi_4Ti_3O_{12}$ sublayers. The expected internal stresses reorient polar domains and prefer domain orientations in the discrete ferroelectric layers.

DOI: 10.1103/PhysRevB.63.104102 PACS number(s): 77.55.+f, 78.30.−j, 77.80.−e

Currently bismuth-layer perovskite materials attract intensive consideration due to their fatigue-free nature of ferroelectric memories made with Pt electrodes.[1] Nevertheless, their dielectric constant is not high enough to meet the demands of integrated circuitry. Theoretical calculation gives an insight into the large electric permittivity expected on ultrathin ferroelectric epitaxial films patterned with periodic ferroelastic domain walls,[2] and a phenomenological thermodynamic theory of ferroelectric thin films predicts ''misfit-temperature'' phase diagrams (ferroelectric and structural) in a single layer under mechanical boundary conditions.[3] Experimentally, the abnormal domain growth was indeed observed even on the strained $PbTiO_3/BaTiO_3$ superlattices,[4] which provided the possibility of artificially constructing domain patterns on multilayers with properties superior to those of the constituents. The importance of periodic domain wall patterns resides not only in the improvement of electric properties, but also in nonlinear optical modulation and phase shift applications.

A major obstacle of dynamic random access memory (DRAM) applications is imprint failure, the preference of one polarization state over the other, which eventually leads to a failure during retrieving the data stored. To overcome it, main concerns have been given from the choice of appropriate electrode materials[5] without considerations of the film structure, possibly due to less understanding of intrinsic microscopic causes.

In this paper, we show the enhanced dielectric permittivity in epitaxial $x\,Bi_2Ti_4O_{11}$-$(1-x)Bi_4Ti_3O_{12}$ (BST) films at the morphotropic phase boundary (MPB) with artificially controlled domain patterns. The antiparallel domain configuration is induced by internal stresses created by the different symmetry phases of constituent $Bi_4Ti_3O_{12}$ in adjacent ferroelectric layers.

All BST films with $LaNiO_3$ (LNO) bottom electrodes were grown epitaxially on single-crystal (100) $SrTiO_3$ (STO) substrates at 750 °C by pulsed excimer laser deposition (PLD) using a single sintered ceramic target. Highly densified BST ceramic targets were prepared by sintering compacted $Bi_2Ti_4O_{11}$ and $Bi_4Ti_3O_{12}$ nanocrystallites with various compositions (in weight).[6] The major advantage of PLD for the synthesis of multicomponent oxide film arises from its intrinsic ability of faithfully transferring the stoichiometry of the target to the film. The top Pt electrodes were vacuum evaporated on films at 400 °C through a shallow mask with the dot area of 3.1×10^{-4} cm^2. The films on (100) MgO substrates were also grown under same deposition conditions for Raman-scattering experiments. The film thickness is about 500 nm. X-ray diffractometry methods (2θ scan, rocking curve, and x-ray pole figure) were used to characterize the film structure. The film capacitance and dielectric loss were measured on multifrequency 4274A and 4275A Hewlett Packard impedance analyzers at room temperature. Raman spectra of the films were recorded on Renishaw 1000 in backscattering geometry using a microprobe device.

X-ray diffractometry measurements show epitaxially grown films with their *c* axes normal to the substrates. X-ray diffraction (XRD) patterns in Fig. 1(a) clearly indicate that the $Bi_2Ti_4O_{11}$ film is composed of double phases of monoclinic TiO_2 and $Bi_4Ti_3O_{12}$. With decreasing $Bi_2Ti_4O_{11}$ con-

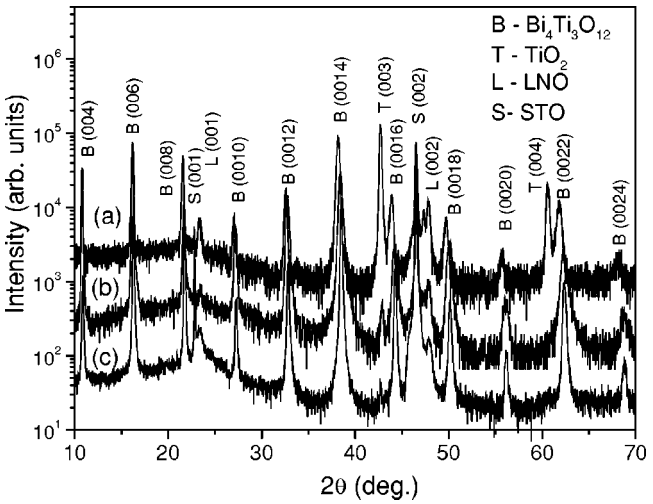

FIG. 1. XRD patterns at room temperature for $x\,Bi_2Ti_4O_{11}$-$(1-x)Bi_4Ti_3O_{12}$ films on LNO electroded STO substrates at (a) $x=1$, (b) $x=0.39$, and (c) $x=0.12$.

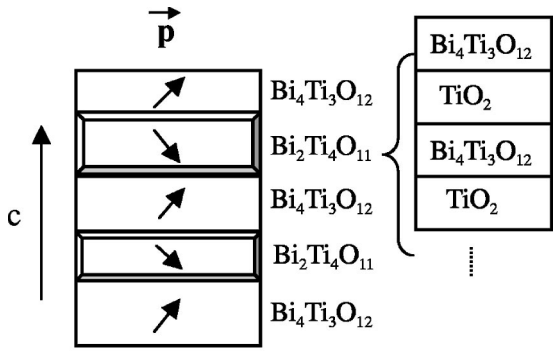

FIG. 2. The schematic diagrams of structural and domain patterns of ferroelectric BST films along the *c* axis.

centration in BST films, the (003) TiO_2 reflection becomes weak in Fig. 1(b), and almost disappears from Fig. 1(c). Coincidently, the pole figure of constituent $Bi_4Ti_3O_{12}$ in BST/STO films shows fourfold (117) reflections at $\beta=0°$, 90°, 180°, and 270° with $\alpha\approx 40°$. The epitaxial growth of $Bi_4Ti_3O_{12}$ and $Bi_2Ti_4O_{11}$ components suggests that BST films are alternative stacking of $Bi_4Ti_3O_{12}$ and $Bi_2Ti_4O_{11}$ layers, as shown by a schematic diagram in Fig. 2.

The film morphology was characterized by atomic force microscopy (AFM) in contact mode. The grains in $Bi_2Ti_4O_{11}/SrTiO_3$ films present a needlelike shape, similar to $Bi_2Ti_4O_{11}$ single crystals,[7] and order highly in two perpendicular directions, as will be reported in paper separately. With increasing $Bi_4Ti_3O_{12}$ concentration, the needlelike grains transform into a platelike shape[8] and the film density increases.

Figure 3 shows the frequency-dependent dielectric response. The dielectric constant ϵ in $Bi_2Ti_4O_{11}$ is about 80 and essentially independent of frequency below 4 MHz. The dielectric constant in BST films increases largely with the elevated $Bi_4Ti_3O_{12}$ concentration at $x=0.39$, then decreases with further increasing $Bi_4Ti_3O_{12}$ composition, such as $\epsilon=639$ with $x=0.39$ and 260 with $x=0.12$ at 10 kHz. In response, the corresponding dielectric loss $\tan\delta$ increases

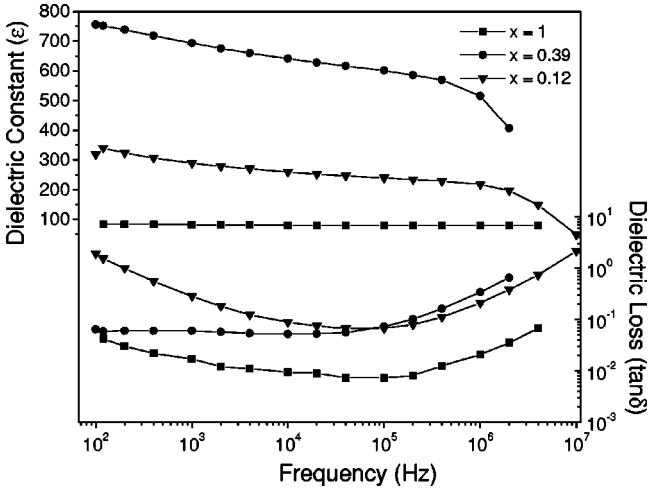

FIG. 3. Frequency dependence of dielectric constant ϵ and loss $\tan\delta$ for $x\ Bi_2Ti_4O_{11}$-$(1-x)Bi_4Ti_3O_{12}$ films at room temperature.

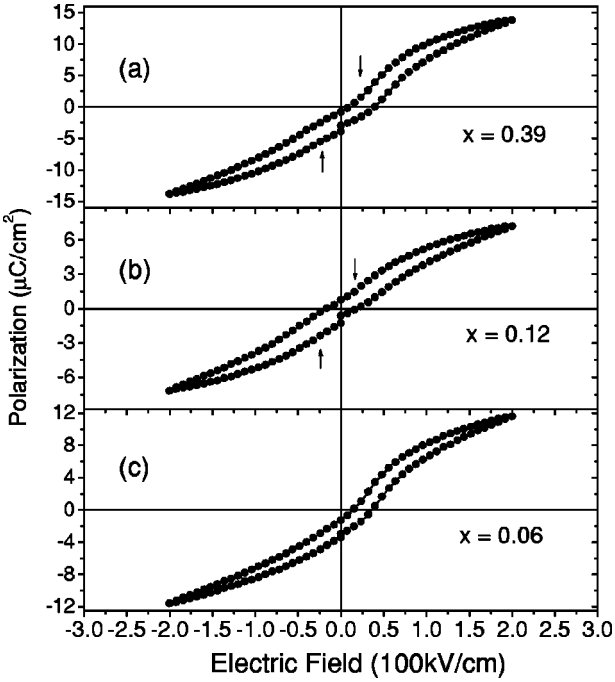

FIG. 4. P-E hysteresis loops for $x\ Bi_2Ti_4O_{11}$-$(1-x)Bi_4Ti_3O_{12}$ films at 67 Hz.

slightly. Though the dielectric constant in $Bi_4Ti_3O_{12}$ film is unknown here due to the high leakage current density on the LNO electrode, it is not higher than 184 according to the report in Ref. 9. Thus, the dielectric constant in the BST film at $x=0.39$ is significantly larger than their constituents, similar to the behavior reported on ferroelectric $BaTiO_3/SrTiO_3$ superlattices.[10]

Ferroelectric hysteresis loops were measured using Radiant technologies RT6000S tester at 67 Hz. Figure 4(a) shows a pseudoantiferroelectric hysteresis loop, evidenced by weak double shoulders (indicated by arrows) at low fields, for the BST film at $x=0.39$ with a saturation polarization $P=9.83\ \mu C/cm^2$, which is higher than the 4 $\mu C/cm^2$ measured on a *z*-cut $Bi_4Ti_3O_{12}$ crystal. The pseudoantiferroelectric character slightly weakens in Fig. 4(b) at $x=0.12$, and almost disappears from Fig. 4(c) at $x=0.06$. At the same time, the ferroelectric property still exists and imprint failure is obvious in Fig. 4(c), in agreement with previous studies on $Bi_4Ti_3O_{12}$.[5] Capacitance versus voltage (*C-V*) measurements in Figs. 5(a)–5(c) further ensure the pseudoantiferroelectric character. There are two peaks biased at internal fields of -33 and $+44$ kV/cm, respectively, with each *C-V* curve, and the peak intensity at -33 kV/cm weakens gradually with decreasing $Bi_2Ti_4O_{11}$ concentration from Figs. 5(a)–5(c). Meanwhile, the peak at $+44$ kV/cm becomes more preeminent, though it seems to collapse in Fig. 5(b) due to inhomogeneous defect pinning. The peak collapse at Fig. 5(b) disappears quickly after cycling the capacitor at ± 10 V several times. The doublet in each *C-V* curve strongly suggests the antiparallel domain patterns in BST multilayers. The peak biased at negative field, which disappears at $x=0$, should originate from the domain reversal in $Bi_2Ti_4O_{11}$ layers, and the other at positive field is due

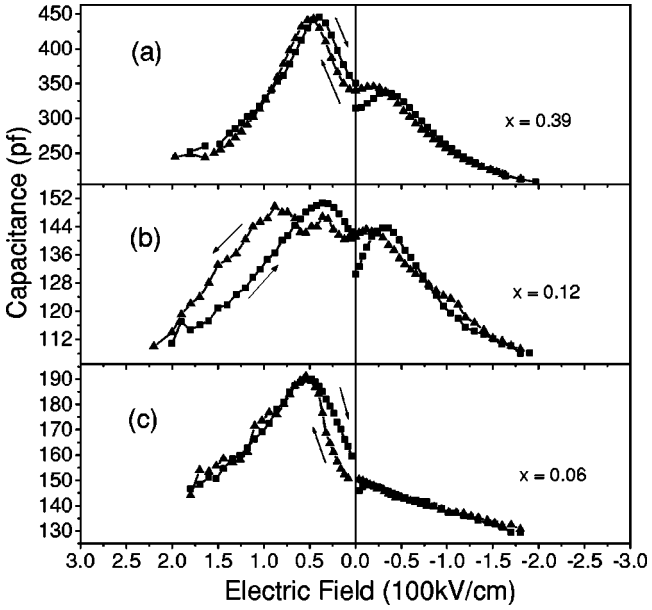

FIG. 5. *C-V* curves for $x\,Bi_2Ti_4O_{11}$-$(1-x)Bi_4Ti_3O_{12}$ films at 10 kHz.

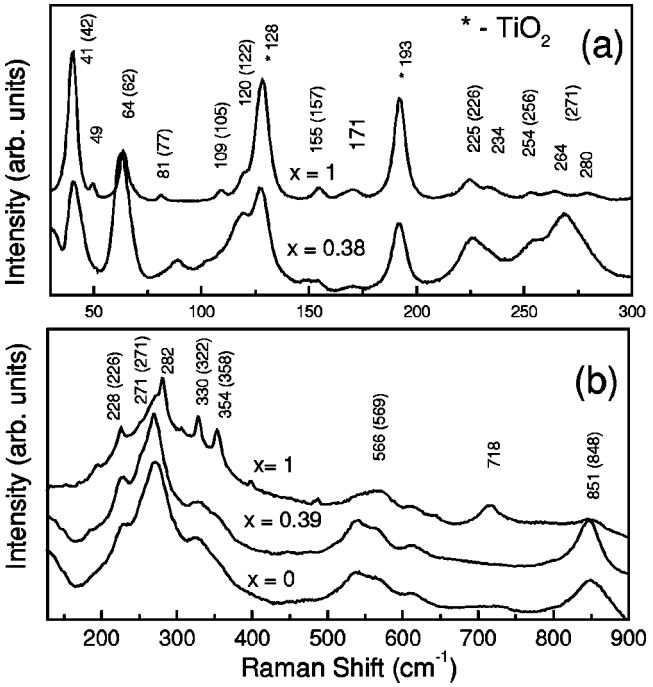

FIG. 6. Raman spectra for (a) $x(La_{0.26}Bi_{0.74})_2Ti_4O_{11}$-$(1-x)Bi_4Ti_3O_{12}$ ceramics and (b) $x\,Bi_2Ti_4O_{11}$-$(1-x)Bi_4Ti_3O_{12}$ films on MgO substrates at room temperature. The wave numbers in parentheses are taken from Ref. 11.

to antiparallel domain switching in $Bi_4Ti_3O_{12}$ layers. The internal bias almost makes the whole capacitor self-poling in Fig. 5(c). Possible dipole orientations with adjacent ferroelectric layers are schematically depicted in Fig. 2 with a pseudoantiferroelectric component along the *c*-axis. The antiferroelectric character is conjectured on a mesoscopic scale comparable to stacking layer thickness instead of a genuine antiferroelectric on a molecular or a microscopic scale.

Raman results either on BST ceramics or on films coincidently indicate the different symmetry phases of constituent $Bi_4Ti_3O_{12}$ in $Bi_2Ti_4O_{11}$ and $Bi_4Ti_3O_{12}$ stacking layers at room temperature, as shown in Figs. 6(a),6(b). $Bi_4Ti_3O_{12}$ is orthorhombic at room temperature, and its Raman lines are usually broad. Below 150 K, the Raman lines become much sharper and more intense, which suggests a monoclinic symmetry phase.[11] Figure 6(a) shows the Raman spectra of $x(La_{0.26}Bi_{0.74})_2Ti_4O_{11}$-$(1-x)Bi_4Ti_3O_{12}$ ceramics (here La modification can avoid ceramic crack and increase bulk density). The Raman active modes for monoclinic TiO_2 constituent can be indexed on the basis of the TiO_2 brookite.[12] The discrete Raman lines for the $Bi_4Ti_3O_{12}$ constituent at $x=1$ is sharp which suggests the low-temperature monoclinic symmetry phase stabilized at room temperature. With increasing $Bi_4Ti_3O_{12}$ concentration, the Raman lines for the constituent $Bi_4Ti_3O_{12}$ at $x=0.38$ are broad and the relative peak intensity changes abnormally due to the increased orthorhombic $Bi_4Ti_3O_{12}$ concentration. Similar results occur with BST/MgO films in Fig. 6(b), which can rule out the possibility of constituent $Bi_2Ti_4O_{11}$ phase change during film fabrication processing. Note that the Raman peaks for the monoclinic TiO_2 are very weak in films. The Raman peaks in $Bi_4Ti_3O_{12}$/MgO are indeed broad, but become much sharper with increasing $Bi_2Ti_4O_{11}$ concentration until $x=1$, such as the modes at 228, 271, 282, 330, 354, and 718 cm^{-1} (it is possible that the new mode at 282 cm^{-1} with $x=1$ originates from the monoclinic TiO_2), which predicts the monoclinic symmetry phase of $Bi_4Ti_3O_{12}$ in $Bi_2Ti_4O_{11}$ sublayers different from the symmetry phase of orthorhombic $Bi_4Ti_3O_{12}$ layers, in agreement with the bulk ceramics.

It is expected that the different symmetry phases of constituent $Bi_4Ti_3O_{12}$ within adjacent $Bi_2Ti_4O_{11}$ and $Bi_4Ti_3O_{12}$ layers induce the large internal stresses which promote in-plane domain reorientations.[3] The antiparallel domain patterns would seem to be the result of the changing energy balance between the elastic strains and the polarization, which contributes considerably to the dielectric permittivity, since the region with the ''unsaturated'' domain wall is held to have a larger dielectric response.[13] With the reduced $Bi_2Ti_4O_{11}$ concentration in BST films, the ''unsaturated'' region decreases linearly. In response, the dielectric constant in Fig. 3 consequently reduced. This finding is favorable for artificial tailoring of ferroelectric dielectric permittivity by controlling antiferroelectric domain patterns, and very important for the commercialization of microelectronic devices.

Imprint failure in Fig. 4(c) induced by an internal bias E_{int} is usually provided by the defect charges inside the ferroelectric materials, the work function difference between top and bottom electrodes, and charges presented at ferroelectric-electrode interfaces. The effect of interfacial charges on imprint failure of epitaxial $Bi_4Ti_3O_{12}$ films has been discussed in detail in Ref. 5 with various top and bottom electrodes, but the influence of internal stresses is seldom reported. It is not so difficult to determine that the internal biases in BST films are opposite with adjacent epitaxial $Bi_4Ti_3O_{12}$ and $Bi_2Ti_4O_{11}$ layers under identical conditions from Figs. 5(a)–5(c). The different symmetry phases of $Bi_4Ti_3O_{12}$ within the adjacent

layers create a large internal stress which stabilizes the reoriented polar domains within discrete ferroelectric layers from the viewpoint of the changing energy balance, and thus the polarization of a capacitor under an external cycling field is preferred. With the reduction of $Bi_2Ti_4O_{11}$ concentration in BST films, the predominant lattice mismatch between bottom electrode and film, as well as the interfacial charge, polarizes the whole capacitor and also pins domain walls, and hence the ferroelectric hysteresis loop in Fig. 4(c) is asymmetric. It should be pointed out that the opposite internal biases with adjacent $Bi_4Ti_3O_{12}$ and $Bi_2Ti_4O_{11}$ layers eliminate the voltage offset of the whole capacitor due to the pseudoantiferroelectric domain patterns in Figs. 4(a) and 4(b), which supplies an effective way to overcome the imprint failure during ferroelectric memory applications.

To summarize, we developed epitaxial $x\,Bi_2Ti_4O_{11}$-$(1-x)Bi_4Ti_3O_{12}$ multilayers with the pseudoantiferroelectric domain patterns in adjacent ferroelectric layers. A large dielectric constant was observed at $x=0.39$. The Raman investigations at room temperature indicate the different symmetry phases of constituent $Bi_4Ti_3O_{12}$ within $Bi_2Ti_4O_{11}$ and $Bi_4Ti_3O_{12}$ stacking layers in BST films. The expected large internal stresses not only reorient the polar domains within discrete $Bi_4Ti_3O_{12}$ and $Bi_2Ti_4O_{11}$ layers, but also prefer domain orientations. The opposite internal biases within adjacent ferroelectric layers minimize imprint failure of the whole capacitor. The generic method is very important in the manufacture of DRAM devices.

This work was supported by a grant for State Key Program of China.

[1] C. A-Paz de Arauzo, J. D. Cuchiaro, L. D. McMillan, M. C. Scott, and J. F. Scott, Nature (London) **374**, 627 (1995).
[2] N. A. Pertsev, G. Arlt, and A. G. Zembilgotov, Phys. Rev. Lett. **76**, 1364 (1996).
[3] N. A. Pertsev, A. G. Zembilgotov, and A. K. Tagantsev, Phys. Rev. Lett. **80**, 1988 (1998).
[4] F. L. Marrec, R. Farhi, M. E. Marssi, J. L. Dellis, and M. G. Karkut, Phys. Rev. B **61**, R6447 (2000).
[5] B. H. Park, T. W. Nch, J. Lee, C. Y. Kim, and W. Jo, Appl. Phys. Lett. **70**, 1101 (1997).
[6] A. Q. Jiang, Z. X. Hu, and L. D. Zhang, J. Appl. Phys. **85**, 1739 (1999).
[7] S. Shimada, K. Kodaira, and T. Matsushita, J. Cryst. Growth **41**, 317 (1977).
[8] C. D. Theis, J. Yeh, D. G. Schlom, M. E. Hawley, G. W. Brown, J. C. Jiang, and X. Q. Pan, Appl. Phys. Lett. **72**, 2817 (1998).
[9] P. C. Joshi and S. B. Desu, J. Appl. Phys. **80**, 2349 (1996).
[10] H. Tabata, H. Tanaka, and T. Kawai, Appl. Phys. Lett. **65**, 1970 (1994).
[11] H. Idink, V. Srikanth, W. B. White, and E. C. Subbarao, J. Appl. Phys. **76**, 1819 (1994); J. F. Meng, P. S. Dobal, R. S. Katiyar, and G. T. Zhou, J. Raman Spectrosc. **29**, 1003 (1998).
[12] G. A. Tompsett, G. A. Bowmaker, B. P. Cooney, J. B. Metson, K. A. Rodgers, and J. M. Seakins, J. Raman Spectrosc. **26**, 57 (1995).
[13] R. Clarke and J. C. Burfoot, J. Phys. D **8**, 1115 (1975).